FSL-LVLM: Friction-Aware Safety Locomotion using Large Vision Language Model in Wheeled Robots

Bo Peng[1*], Donghoon Baek[2], Qijie Wang[3], and Joao Ramos[1,2]

Abstract— Wheeled-legged robots offer significant mobility and versatility but face substantial challenges when operating on slippery terrains. Traditional model-based controllers for these robots assume no slipping. While reinforcement learning (RL) helps quadruped robots adapt to different surfaces, recovering from slips remains challenging, especially for systems with few contact points. Estimating the ground friction coefficient is another open challenge. In this paper, we propose a novel friction-aware safety locomotion framework that integrates Large Vision Language Models (LVLMs) with a RL policy. Our approach explicitly incorporates the estimated friction coefficient into the RL policy, enabling the robot to adapt its behavior in advance based on the surface type before reaching it. We introduce a Friction-From-Vision (FFV) module, which leverages LVLMs to estimate ground friction coefficients, eliminating the need for large datasets and extensive training. The framework was validated on a customized wheeled inverted pendulum, and experimental results demonstrate that our framework increases the success rate in completing driving tasks by adjusting speed according to terrain type, while achieving better tracking performance compared to baseline methods. Our framework can be simply integrated with any other RL policies.

I. INTRODUCTION

Wheeled-legged robots combine the speed of wheels with the adaptability of legs, making them ideal for applications from industrial automation to disaster response [1], [2], [3]. Recent studies show that both model-based [2], [4] and RL-based locomotion controllers [5], [6], [7], [8], [9], [10] enable legged robots to handle challenging terrains. Model-based methods offer predictability and interpretability but rely on accurate dynamics and require tuning, while RL-based methods adapt well to complex environments but are sample inefficient and less interpretable. Hybrid approaches that combine both methods have been explored to leverage their strengths and mitigate individual drawbacks [11], [12], [13].

Despite the promising results in legged robot locomotion, controlling a wheeled-legged robot on harsh terrain remains a significant challenge. Specifically, on slippery surfaces, slipping can cause a system to quickly lose controllability and fall over. Recovery is particularly challenging for bi-wheeled robots due to their limited degrees of freedom and contact points, which physically restrict their ability to make the necessary adjustments to stabilize and regain balance.
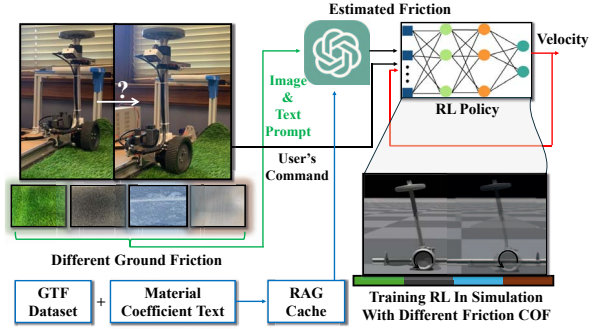
Fig. 1: **Overview of Friction-Aware Safety Locomotion Framework using Large Vision Language Model (FSL-LVLM).** This shows how a Large Vision Language Model integrates with a RL policy to control a wheeled robot on slippery surfaces. The Friction-from-Vision (FFV) module estimates ground friction using image and text data, enabling the RL policy to adapt behavior based on friction coefficients before contact. Developed in simulation, the pre-trained policy transfers successfully to the real world without manual tuning.

Moreover, once slipping begins, the frictional force decreases because the kinetic Coefficient of Friction (COF) is usually smaller than static COF. This reduced frictional force means the robot has less resistance to counteract slipping, making recovery and control more challenging. Interestingly, humans leverage their past experiences and sensory memories to adjust their behavior before reaching the new situation.

In this work, we propose a Friction-aware Safety Locomotion framework (FSL-LVLM) that enables a wheeled-legged robot to avoid slipping by leveraging a friction-from-vision (FFV) module for improved decision-making using a Large Vision Language Model. The idea is inspired by how humans adjust their actions in advance through visual judgment when approaching a slippery surface. For wheeled systems like wheeled inverted pendulums and wheeled humanoids, we suggest prioritizing slip avoidance over real-time recovery to maintain stability. The key technical challenge lies in estimating the ground friction coefficient from visual information, especially given the limited availability of datasets. To address this issue, We propose using a large vision language model (LVLM) to estimate the ground friction coefficient, eliminating the need for large datasets and extensive training, and explicitly incorporating this information into a RL policy. We found that LVLM effectively estimates the COF by incorporating various factors and semantic information. Additionally, we observed that an RL policy performs better when the estimated friction coefficient is explicitly incorporated, enabling it to more effectively adapt to ground conditions.

II. RELATED WORKS

A. Large Vision Language Models (LVLMs).

Multimodal Large Language Models (MLLMs) represent a major advancement in AI, allowing models to process diverse data types like text, images, and audio [14], [15], [16], [17], [18]. Large Vision Language Models (LVLMs), a subset of MLLMs, excel in visual-language reasoning tasks, often achieving impressive zero-shot and few-shot performance with minimal training.

B. Estimating Friction from Vision.

Estimating ground friction remains a challenge without a universal solution. Humans often assess slipperiness through visual cues like surface gloss and roughness, though these perceptions can be imprecise [19], [20]. Variations in image intensity suggest rough surfaces, correlating with higher friction. Some methods predict friction by identifying surface types and referencing known databases [21], but these are limited by the lack of a comprehensive friction-vision dataset and environmental factors. Inspired by [22], which used text mining to infer COF, we propose leveraging LVLMs' strong generalization and reasoning abilities with visual data to estimate COF across surfaces.

C. Legged Robot Locomotion.

Recent research on quadruped locomotion highlights robustness and agility, focusing on navigating difficult terrains and performing parkour-like tasks [6], [7], [23], [24], [25]. Similarly, humanoid locomotion has been extensively studied using both model-based and model-free methods [26], [27], [28], [29], [30]. Anticipating environmental challenges is crucial for robots to avoid accidents and improve task performance. For example, incorporating visual information increased success rates in stair climbing from 40% to 100% [8], and bipedal robots have been shown to select less slippery paths for safer navigation [21]. This highlights the importance of integrating environmental factors into RL to prevent slips and enhance safety. Recent work also addresses locomotion on slippery ground but requires extensive training [31].

III. METHODS

The proposed ground friction-aware locomotion framework, FSL-LVLM, comprises two key components: 1) the Friction-from-Vision (FFV) module, which uses an LVLM to estimate the ground friction coefficient (f_t) from images, and 2) an RL policy trained entirely in simulation, then transferred to the real world with zero-shot learning. The procedure of our framework is shown in Fig. 1.

A. Friction-from-Vision: Estimating the Ground-Friction Coefficient using Large Vision Language Model

We introduce the FFV module, which employs a selected LVLM to estimate the COF of the ground. We chose *GPT4-o* due to its performance and convenient API. Enhancing LVLMs for a specific task when the robot wheels or feet is fixed involves several approaches, ranked in terms

of modification to LVLMs: training from scratch on a specialized dataset, fine-tuning [32], Retrieval-Augmented Generation (RAG) [33], and prompt engineering. While retraining and fine-tuning yield promising results, they demand large-scale datasets, which are currently lacking. To address this limitation, we employ RAG with an open-source dataset, supplemented by 94 text-based friction coefficient references [34], [35]. The dataset used is the *Ground-Truth coefficient of Friction dataset* (GTF) [22], comprising 129 images of 43 walkable surfaces.

For each walkable surface in the GTF, we utilized a pre-trained CLIP visual encoder to encode the original image $x_i, i \in N$, where N is the total number of surfaces, into features $f_{\text{img}}^i \in \mathbb{R}^D, i \in [1, N]$, D represents the dimension of the CLIP features. The format of the text friction coefficient data is similar to:

```
"Material": "Wrought iron",
"Static Coefficient of Friction": 0.44,
"Against Material": "wrought iron"
```

For each piece of data, we construct a simple prompt t_i as "[Material] and [Against Material]", $i \in M$, where M is the number of text friction coefficient data entries, and use the pre-trained CLIP text encoder to encode t_i into features $f_{\text{text}}^i \in \mathbb{R}^D, i \in [1, M]$. Subsequently, pairs of image feature-image path and text feature-text are cached in a cache file. For the input image y, we still use the CLIP visual encoder to encode its features as f_y. We read all f_x and f_{text} from the cache file. Then they are concatenated into two matrices, $F_{\text{img}} \in \mathbb{R}^{N \times D}$ and $F_{\text{text}} \in \mathbb{R}^{M \times D}$. We calculate the cosine similarity between f_y and F_{text}, and between f_y and F_{img},

$$\text{cosine\_similarity}(f_y, F_{\text{text}}) = \frac{f_y \cdot F_{\text{text}}^T}{\|f_y\|\|F_{\text{text}}\|}$$
$$\text{cosine\_similarity}(f_y, F_{\text{img}}) = \frac{f_y \cdot F_{\text{img}}^T}{\|f_y\|\|F_{\text{img}}\|} \quad (1)$$

taking the top K as cached knowledge from the image and text caches, and input them together with the input prompt into GPT4 Vision. The input prompt defines the format of the text returned by GPT4 Vision, so the estimated COF value can be obtained using regular matching in the text returned by GPT4 Vision.

B. Friction-Aware Reinforcement Learning

Using history of proprioception as an observation in RL policies has become a standard approach in legged robot control [6], [7], [23], [24], [25]. The underlying assumption is that proprioceptive data contains enough information to replace privileged parameters such as ground friction. The inherent limitation of this method is that it requires the robot to experience new situations for the proprioception history to capture meaningful data. While this can be done in real-time, for systems with limited ground contact points, reacting and recovering is particularly challenging. A good example is to imagine a human wearing wheeled skates,

trying to regain balance to avoid falling—such recovery. For this reason, we decided to explicitly incorporate an estimated ground friction coefficient in the RL policy, rather than relying solely on the robot's proprioception. We trained the RL policy separately from a LVLM in simulation. To consider the LVLM's estimation error, we introduced Gaussian noise and random estimation errors in the estimated value, which was then fed into the RL policy.

Observation. Having more information does not always mean better performance. Some of it may be redundant and sometimes even increases the *reality gap* [36]. In a classical approach, slipping in the WIP system is examined in [37], where the absolute slip γ is defined as $\frac{r\dot{\alpha}-\dot{x}}{2\pi r}$. Here, r is a wheel radius, $\dot{\alpha}$ is the angular velocity, and $\dot{x}$ is the linear velocity. The extended equation for calculating friction is $\hat{f} = \mu \text{sign}(\gamma)$ where μ is the friction coefficient. Inspired by this, we designed our observation space as follows:

$$o_t = \{x_w, \dot{x}_w, \beta, \dot{\beta}, x_{tr}, a_{t-1}, c_t, \hat{\mu}\} \qquad (2)$$

where, x_w and $\dot{x}_w$ represent the angular position and velocity of the wheel, while β and $\dot{\beta}$ denote the angular position and velocity of the pole joint. The variable a_{t-1} is the previous action, c_t is the user command, and $\hat{\mu}$ is the estimated friction from the LVLMs. Additionally, x_{tr} refers to the position of the translation joint. It is important to note that x_{tr}, a translation joint, is not accessible in the real world and is not accurate even if visual odometry is used. When there's a sudden change in x_{tr}, we cannot tell whether it's caused by slipping or sensor noise, making this information unreliable. But we observed that including x_{tr} in the observation space improves the tracking performance and stability during RL policy training. This is because the x_{tr} provides the RL policy with additional information about slip, given the significant disparity between x_{tr} and x_w, which are nearly identical under normal conditions. As a training trick, we initially used x_{tr} and construct the reward function to reduce the disparity between x_{tr} and x_w so the policy is trying to learn to "avoid slipping". When the reward value converges and the performance is stable, wse substitute the x_{tr} with x_w in the deployment stage.

Action Space. The action a_t represents the desired velocity for the wheel joint. Empirically, we found that using velocity mode with a built-in PD controller ($k_p = 0, k_d = 3$) leads to faster training convergence and simplifies sim-to-real transfer compared to directly learning the torque.

Reward Function. The reward function is designed considering the five major components as follows.

$$R_t = \underbrace{1 - \beta_t^2}_{\text{Keep balance}} \underbrace{- 0.01|\dot{x}_t| + 0.005|\dot{\beta}_t|}_{\text{Penalty for oscillation}} \underbrace{- 3|\dot{x}_t - r\dot{\alpha}_t|}_{\text{Avoid Slipping}}$$
$$+ \underbrace{\frac{0.3\zeta_t}{e_t + 0.01}a_{j,t}^2}_{\text{Tracking Component}} \underbrace{- (A_l + (A_h - A_l)\zeta_t)a_{j,t}^2}_{\text{Output penalty}} \qquad (3)$$

This encourages the system to track the desired velocity while maintaining stability and preventing slip. Since we use a single actuator to balance and track the signal, producing smooth outputs is crucial for effective sim-to-real transfer. The output penalty term is designed to penalize actions that apply excessive force or velocity in the system, ensuring smoother control. The A_l and A_h are two predefined parameters, the lowest output penalty and the highest output penalty, respectively. We observed that incorporating the "avoiding slipping" term significantly enhances tracking performance.

Curriculum Learning. In the reward function (3), the term ζ_t contributes to curriculum learning and is defined as follows.

$$\zeta_t = (tanh(\bar{T}_t/T_{max} * 8 - 3) + 1)/2 \qquad (4)$$

where $\bar{T}_t$ is the current mean episode length and T_{max} is the maximum episode length. Initially, the focus of the training process is on learning balancing, gradually transitioning attention towards the tracking task. The $tanh$ function ensures that this parameter increases slowly during the early stages of training, allowing the policy to focus on easier tasks.

IV. EXPERIMENTS

A. Customized Wheeled-Inverted Pendulum

A customized Wheeled-Inverted Pendulum (WIP) was developed to verify the proposed framework's feasibility, as shown in Fig. 2(a, b). This system is a simplified version of the wheeled humanoid robot, SATYRR [1]. Unlike the traditional inverted pendulum, our WIP system includes a wheel joint and a roll joint, causing irregular ground contact and making control more challenging. For example, when the wheel accelerates aggressively, it often lifts off and loses contact with the ground.

B. Simulation and Hardware details

Hardware Setup. The system employs the same actuators as a wheeled humanoids [3], with an inertial measurement unit (VN-100, VectorNav, USA) mounted on the pole link. We used a RealSense (D405 model) camera to obtain the
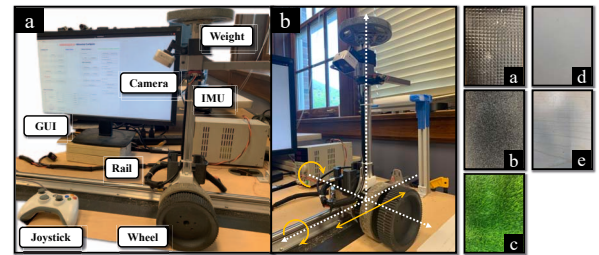

Fig. 2: **The experiments involve testing two types of wheels (smooth and rough) across five surfaces (rubber, anti-slip tape, wood, cardboard, and grass).** The smooth wheel is tested on wood, cardboard, and grass, while the rough wheel is tested on rubber and anti-slip tape. Each wheel-surface combination forms a distinct testing environment. For accurate evaluation, three tests are conducted for each combination, resulting in a total of 15 tests.

Model	Network	Model	Network
Actor	FC (10, 64) Lrelu FC (64, 64) Lrelu FC (64, 1)		Conv1d Length = 40 Num of Kernels = 64 Kernel Size = 3 Stride = 1
Critic	FC (10, 64) Lrelu FC (64, 64) Lrelu FC (64, 1)	Adaptation Module	Padding = 1 FC(2560, 256) Relu FC(256, 64) Relu
Environment Encoder	FC (1, 2) Lrelu FC (2, 1)		FC(64, 8) Relu FC(8, 1)

TABLE I: **Architecture of PPO and RMA.** The symbol $FC(a, b)$ denotes a fully connected layer with input dimension a and output dimension b. The term $Lrelu$ refers to the leaky ReLU. We adopted this architecture for both our method and all baseline approaches.

ground images. Five different types of surface materials are used in the real-world tracking task. The control loop runs at 400 Hz, and the RL policy's decision frequency is 50 Hz. All software is connected via the Robot Operating System.

Simulation Environment Setup. We utilize the IsaacGym (IG) simulator to train our RL policy and all baselines for customized wheeled inverted pendulum (WIP). Unified Robot Description Format (URDF) [38] file is employed to simulate a customized wheeled inverted pendulum. We configure the static and dynamic friction of the ground to be 0, and we adjust the friction condition of the WIP's wheel accordingly. IsaacGym calculates the COF between two surfaces as the average of the COFs of each surface.

C. Experimental Plan

The experiments aim to: 1) validate the friction estimation performance of the FFV module; 2) assess how effectively our framework completes the tracking task without failure across various surface types compared to baseline methods; and 3) analyze the impact of incorporating privileged information (translation joint) into the observation space.

Ground Friction Coefficient Estimation of FFV Module. We employed the GTF dataset [22] to evaluate the estimation performance of the FFV module, using Residual Mean Squared Error (RMSE) as evaluation indices. Same as [22], we validated our algorithm by using 2, 5, and 10 fold cross validation. For the baseline, Vision Transformer (ViT) [39] and Word Material-Material similarity (WordMM) [22] assuming perfect segmentation are used.

Safety Driving Performance Evaluation. We conducted safety driving tasks both in simulation and in the real world using our customized wheeled inverted pendulum. For a system with few degrees of freedom (DOFs) and contact points, driving more cautiously can improve task success rates. Consequently, we prioritize success rate as our primary evaluation criterion, while also assessing the tracking performance of our method and baseline approaches. For the baselines, the classical LQR [40], PPO [41], PPO with Domain Randomization [42] and RMA [9] which are commonly used to control wheeled robots are
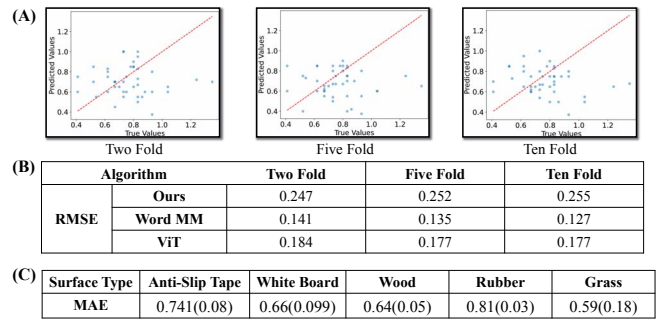

Fig. 3: **Results of Friction Coefficient Estimation.** (A) Cross-validation was employed due to the limited dataset size, with results depicted for 2, 5, and 10-fold validation. (B) Comparison of friction coefficient estimation performance between FFV module and other methods. For the Word MM, we got the result from the paper. (C) Estimation of friction coefficients for various surface types, presented as the mean and standard deviation of ten trials.

(B)

Algorithm		Two Fold	Five Fold	Ten Fold
RMSE	Ours	0.247	0.252	0.255
	Word MM	0.141	0.135	0.127
	ViT	0.184	0.177	0.177

(C)

Surface Type	Anti-Slip Tape	White Board	Wood	Rubber	Grass
MAE	0.741(0.08)	0.66(0.099)	0.64(0.05)	0.81(0.03)	0.59(0.18)

Type	1	2	3	4	5	6	7	8
LVLM	0.6	0.45	0.5	0.35	0.5	0.5	0.8	0.8
VIT	0.75	0.83	0.73	0.85	0.76	0.84	0.65	0.55

Fig. 4: **Friction coefficient estimation results for images with different textures.** Applying oil, grass, or water to the surface increases slipperiness. GPT-4o can recognize these changes and adjust the COF output accordingly, whereas the Vision Transformer lacks this capability.

selected. To implement RMA, the privileged information includes the COF, with the encoder network generating an extrinsic vector z_t of size 1 based on this coefficient.
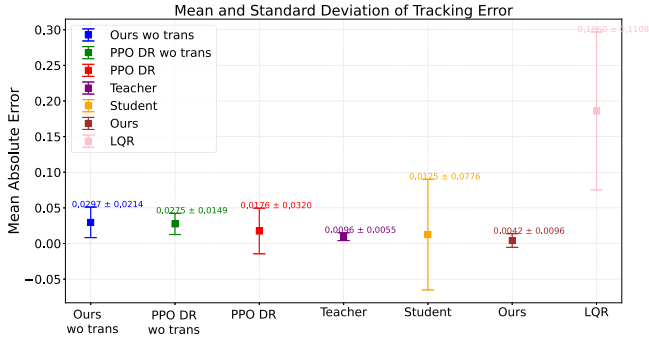
Ablation Study. It is not natural to adopt translation joints as observations because it is difficult to obtain actual values from hardware. As discussed in Section III-B, the difference between the velocity of the translation joint and that of the wheel joint is crucial for detecting slip. In the ablation study, we focus on evaluating the impact of incorporating the translation joint on RL tracking performance in slippery conditions. In addition, we also explore how simple Domain Randomization (DR) [42] can contribute to the anti-slip effect.
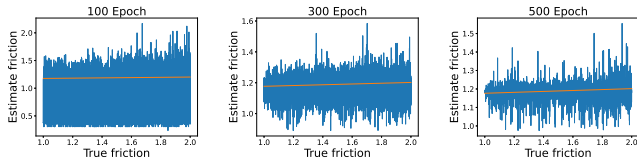
V. RESULTS AND ANALYSIS

A. Friction Coefficient Estimation Results

The friction coefficient estimation result are summarized in Fig. 3. Despite the FFV module with LVLM is not specifically trained for estimating ground friction coefficient, the FFV module shows almost similar performance to a Vision Transformer (ViT) and Word MM. Note that our FFV module achieved comparable COF estimation performance in an end-to-end manner. While quantifying accuracy numerically can be challenging, it provides reasonably accurate values, particularly for materials that are known to be more slippery or rough (see Fig. 3-C).

The FFV module with LVLM demonstrates superior inference ability using text information compared to estimating

Fig. 5: **Comparison Result of Tracking Task in Simulation.** The system begins at zero position with desired position range of [-0.3m, 0.3m]. A single policy is trained for all terrains and evaluated. The mean and standard deviation are calculated from 1,000 results tested across various ground surface types.
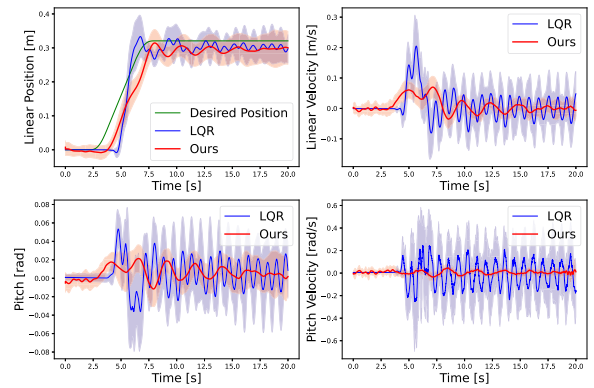

Fig. 6: **Estimated friction from the Adaptation Module in the RMA.** We observed that while the Adaptation Module's output closely follows the pattern of the ground truth friction, it is quite noisy. Originally, the Adaptation Module was not designed to estimate true parameters. This implies that using a deterministic value for the estimated friction is more effective in enhancing the stability and tracking performance of the wheeled robot compared to using a latent vector.

friction solely from images. For instance, while the floor surfaces might appear similar—such as those affected by water, oil, or grass—the actual slipperiness can vary significantly with additional materials. Unlike VIT, which provides the same output regardless of context, the FFV module offer values that account for the effects of additional materials, as illustrated in Fig. 4.

B. Tracking Performance Comparison in Simulation

We report the simulation tracking performance comparison results in Fig 5. The proposed FSL-LVLM attained the smallest tracking error, even outperforming the teacher policy slightly. This suggests that incorporating the friction coefficient into an RL policy is more effective than relying on the encoder network's latent vector. A similar finding is reported in [43], where the estimator is trained directly rather than using a latent vector. The student policy shows significantly higher tracking error variability compared to other methods. We observed that while the adaptation module can reproduce the encoder network using only the robot's proprioception history, the system tends to fall suddenly and cannot recover due to its limited contact points with the ground. This suggests that relying solely on proprioception may not be ideal for learning recovery motions (e.g., RMA) in systems with few degrees of freedom and contact points. Using a Domain randomization can enhance the robustness of a RL policy, but its overall effectiveness is constrained, offering only marginal improvements. Furthermore, we ob-
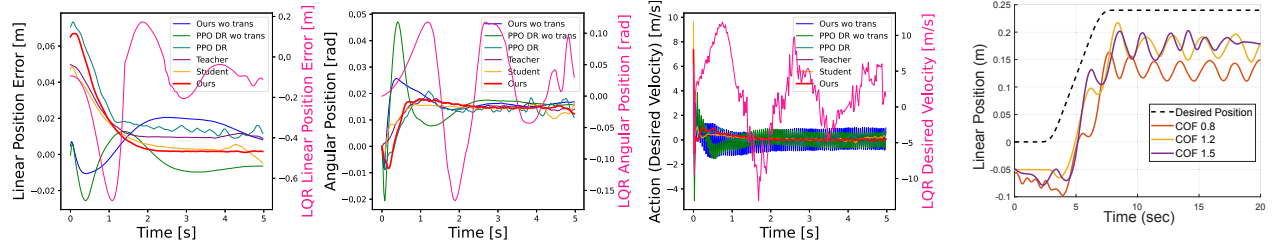

Fig. 7: **Result of Tracking Task in Real World.** We evaluated our framework across combinations of five different ground surfaces and two types of wheel materials in a custom WIP system. The curves show the mean trajectories of only successful cases where the WIP remained stable, with colored areas indicating the standard deviation. Our method successfully completed tracking tasks on all ground surfaces, whereas LQR failed on the most slippery terrain. A smooth fifth-order polynomial trajectory was used as the desired path for the algorithm to track.

served that incorporating a translational joint significantly enhances tracking performance. This is attributed to the fact that relying solely on the wheel joint does not provide sufficient information to accurately capture slip behavior. In the case of LQR, the lack of knowledge about ground friction causes the system to focus solely on minimizing tracking error, which often leads to failure.

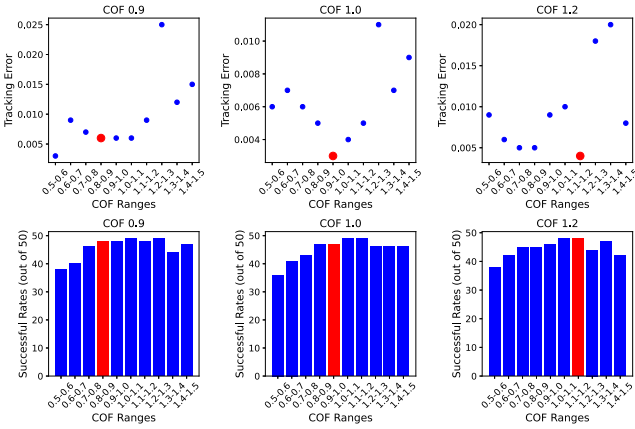### C. Tracking Performance Comparison in Physical System.

The tracking performance results in the real world are presented in Fig. 7, where we observed that only our framework was successfully transferred to the physical system. Other methods, such as PPO and RMA, demonstrated either overly aggressive or conservative behaviors, resulting in oscillations or stationary states. Specifically, for RMA, the output variance, as noted in the simulation, was large, often leading to more aggressive motions. In contrast, domain randomization with PPO tended to produce more conservative actions, like stationary motions, to prevent falls. For systems with slippery surfaces and few contact points, this may not be a surprising result. A good example is to compare standing on one foot versus using both hands and feet to support yourself when rollerblading on slippery terrain. This challenge also lies in how quickly we can detect slip and how fast the system can react. Proprioception, which relies on recording history data, often introduces delays in response. With only a single contact point, the system lacks additional mechanical options to stabilize the robot once slip occurs, making rapid recovery difficult. This highlights the importance of using a Latent Variable Learning Model (LVLM) to predict terrain slipperiness in advance. Compared to LQR, our framework achieved better tracking with less aggressive motion. The LQR-controlled inverted pendulum failed on the most slippery surface, as LQR cannot adapt to varying ground types, while our framework adjusts motion based on surface conditions.

(a) Trajectory Error of Each Methods in Simulation

(b) Performance Difference depending on Input COF in Real World

Fig. 8: **Trajectory Error for Each Method in Simulation and Performance Difference Depending on Input COF in the Real World**. (a) The trajectories represent the mean of successful samples from simulation experiments. Our method (red) achieves the minimum tracking error and generates smooth actions (desired velocity) compared to other methods. Producing smooth actions is crucial for successfully transferring a trained policy to a physical system (see the desired velocity graph). (b) The graph illustrates that our method responds differently based on the input COF, which is the estimated friction coefficient from the FFV module. This enables the system to adjust its motion in response to various ground surfaces before contact.

Fig. 9: **Different Tracking Error and Success Rate Depending on Accuracy of Estimated COF.** This shows that how inaccurate COF estimation affects the tracking performance and success rate. Better estimation performance results in lower tracking errors and higher task success rates. If the estimated COF exceeds the actual COF, the system is likely to fall, resulting in a lower success rate. Conversely, if the actual COF is higher than estimated, tracking performance deteriorates.

We also observed empirically that in a rigid-body simulation, losing point contact can easily occur with minimal contact force because there is no penetration. In our system, slipping occurs easily due to the uncontrollable passive roll joint and slippery ground, leading to instability and the risk of system ejection. This complicates the training process, making it more challenging. This is one reason why classical PPO and Domain Randomization struggled, suggesting that complex designs can pose additional challenges for making RL policies work effectively.

VI. DISCUSSION AND LIMITATIONS

While FSL-LVLM demonstrated superior performance compared to other baselines, there are still several factors that require improvement. Firstly, while our customized wheeled inverted pendulum system is more complex than traditional designs, it remains considerably simpler than wheeled humanoids [1]. However, we believe that FSL-LVLM can maintain its effectiveness and versatility, given its potential

for seamless integration into various other applications. Secondly, the FFV module's estimation speed is relatively slow, primarily constrained by the processing speed of the GPT-4 server. This is the biggest barrier to our methodology updating ground information in real time. However, we believe that this can be improved in the near future. However, unless the ground state changes dramatically in real time, anticipating and adjusting behavior based on the expected ground state can be advantageous in itself. One interesting avenue for future work could involve applying FSL-LVLM to tele-operation scenarios [44], aiming to mitigate human errors by dynamically adjusting the user's commands to accomplish tasks more safely. Thirdly, once the system slips, it disrupts the assumption that the positions of the wheel joint and translation joint are nearly identical, leading to instability. This issue can be mitigated by employing visual odometry [45] and sensor fusion techniques, leveraging camera data unaffected by the wheel joint.

VII. CONCLUSION

In this work, FSL-LVLM, friction-aware safety locomotion framework using large vision language model is proposed. We first introduce the FFV module with LVLM, which can estimate the ground friction coefficient—a parameter that is difficult to measure and for which there is limited dataset availability. Although it still has limitations in real-time performance, it has sufficient utility in that it can predict the risk of the system falling in advance and further improve driving safety by reasonably understanding the ground condition by utilizing texture information, thereby successfully completing driving tasks. We demonstrate the FSL-LVLM both in simulation and in the real world, showing that it enables adaptive behavior in wheeled robots and helps mitigate slip risks across various ground surfaces. Our FSL-LVLM implementation is straightforward and integrates seamlessly with existing RL-based methods without requiring structural changes. We believe our work opens up intriguing research directions, such as exploring whether a VLM can be used to assess terrain properties beyond just friction.

REFERENCES

[1] A. Purushottam, Y. Jung, K. Murphy, D. Baek, and J. Ramos, "Hands-free telelocomotion of a wheeled humanoid," in *2022 IEEE/RSJ International Conference on Intelligent Robots and Systems (IROS)*. IEEE, 2022, pp. 8313–8320.

[2] V. Klemm, A. Morra, L. Gulich, D. Mannhart, D. Rohr, M. Kamel, Y. de Viragh, and R. Siegwart, "Lqr-assisted whole-body control of a wheeled bipedal robot with kinematic loops," *IEEE Robotics and Automation Letters*, vol. 5, no. 2, pp. 3745–3752, 2020.

[3] A. Purushottam, C. Xu, Y. Jung, and J. Ramos, "Dynamic mobile manipulation via whole-body bilateral teleoperation of a wheeled humanoid," *IEEE Robotics and Automation Letters*, 2023.

[4] D. Baek, Y. Sim, A. Purushottam, S. Gupta, and J. Ramos, "Real-to-sim adaptation via high-fidelity simulation to control a wheeled-humanoid robot with unknown dynamics," *arXiv preprint arXiv:2403.10948*, 2024.

[5] A. Agarwal, A. Kumar, J. Malik, and D. Pathak, "Legged locomotion in challenging terrains using egocentric vision," 2022.

[6] J. Lee, J. Hwangbo, L. Wellhausen, V. Koltun, and M. Hutter, "Learning quadrupedal locomotion over challenging terrain," *Science Robotics*, vol. 5, no. 47, Oct. 2020. [Online]. Available: http://dx.doi.org/10.1126/scirobotics.abc5986

[7] J. Hwangbo, J. Lee, A. Dosovitskiy, D. Bellicoso, V. Tsounis, V. Koltun, and M. Hutter, "Learning agile and dynamic motor skills for legged robots," *Science Robotics*, vol. 4, no. 26, p. eaau5872, 2019.

[8] A. Loquercio, A. Kumar, and J. Malik, "Learning visual locomotion with cross-modal supervision," 2022.

[9] A. Kumar, Z. Fu, D. Pathak, and J. Malik, "Rma: Rapid motor adaptation for legged robots," 2021.

[10] A. Kumar, Z. Li, J. Zeng, D. Pathak, K. Sreenath, and J. Malik, "Adapting rapid motor adaptation for bipedal robots," in *2022 IEEE/RSJ International Conference on Intelligent Robots and Systems (IROS)*. IEEE, 2022, pp. 1161–1168.

[11] F. Jenelten, J. He, F. Farshidian, and M. Hutter, "Dtc: Deep tracking control," *Science Robotics*, vol. 9, no. 86, p. eadh5401, 2024.

[12] D. Kang, J. Cheng, M. Zamora, F. Zargarbashi, and S. Coros, "Rl+model-based control: Using on-demand optimal control to learn versatile legged locomotion," *IEEE Robotics and Automation Letters*, 2023.

[13] D. Baek, A. Purushottam, and J. Ramos, "Hybrid lmc: Hybrid learning and model-based control for wheeled humanoid robot via ensemble deep reinforcement learning," in *2022 IEEE/RSJ International Conference on Intelligent Robots and Systems (IROS)*. IEEE, 2022, pp. 9347–9354.

[14] A. Radford, J. W. Kim, C. Hallacy, A. Ramesh, G. Goh, S. Agarwal, G. Sastry, A. Askell, P. Mishkin, J. Clark *et al.*, "Learning transferable visual models from natural language supervision," *arXiv preprint arXiv:2103.00020*, 2021.

[15] A. Ramesh, M. Pavlov, G. Goh, S. Gray, C. Voss, A. Radford, M. Chen, and I. Sutskever, "Zero-shot text-to-image generation," *arXiv preprint arXiv:2102.12092*, 2021.

[16] A. Jaegle, F. Gimeno, A. Brock, O. Vinyals, A. Zisserman, and J. Carreira, "Perceiver: General perception with iterative attention," *arXiv preprint arXiv:2103.03206*, 2021.

[17] J.-B. Alayrac, A. Recasens, A. Raichuk, T. Ramalho, Q. de Laroussilhe, P.-E. Mazaré, X. Zhai, M. Michalski, S. Borgeaud, R. Stojnic *et al.*, "Flamingo: a visual language model for few-shot learning," *arXiv preprint arXiv:2204.14198*, 2022.

[18] L. H. Li, M. Yatskar, D. Yin, C.-J. Hsieh, and K.-W. Chang, "Align before fuse: Vision and language representation learning with momentum distillation," in *Proceedings of the IEEE/CVF International Conference on Computer Vision*, 2021, pp. 10 910–10 920.

[19] A. S. Joh, K. E. Adolph, M. R. Campbell, and M. A. Eppler, "Why walkers slip: Shine is not a reliable cue for slippery ground," *Perception & Psychophysics*, vol. 68, pp. 339–352, 2006. [Online]. Available: https://api.semanticscholar.org/CorpusID:9260972

[20] M. F. Lesch, W.-R. Chang, and C.-C. Chang, "Visually based perceptions of slipperiness: underlying cues, consistency and relationship to coefficient of friction," *Ergonomics*, vol. 51, no. 12, pp. 1973–1983, 2008.

[21] M. Brandao, Y. M. Shiguematsu, K. Hashimoto, and A. Takanishi, "Material recognition cnns and hierarchical planning for biped robot locomotion on slippery terrain," in *2016 IEEE-RAS 16th International Conference on Humanoid Robots (Humanoids)*. IEEE, 2016, pp. 81–88.

[22] M. Brandão, K. Hashimoto, and A. Takanishi, "Friction from vision: A study of algorithmic and human performance with consequences for robot perception and teleoperation," in *2016 IEEE-RAS 16th International Conference on Humanoid Robots (Humanoids)*, 2016, pp. 428–435.

[23] T. Miki, J. Lee, J. Hwangbo, L. Wellhausen, V. Koltun, and M. Hutter, "Learning robust perceptive locomotion for quadrupedal robots in the wild," *Science Robotics*, vol. 7, no. 62, p. eabk2822, 2022.

[24] Z. Zhuang, Z. Fu, J. Wang, C. Atkeson, S. Schwertfeger, C. Finn, and H. Zhao, "Robot parkour learning," *arXiv preprint arXiv:2309.05665*, 2023.

[25] X. Cheng, K. Shi, A. Agarwal, and D. Pathak, "Extreme parkour with legged robots," *arXiv preprint arXiv:2309.14341*, 2023.

[26] M. Chignoli, D. Kim, E. Stanger-Jones, and S. Kim, "The mit humanoid robot: Design, motion planning, and control for acrobatic behaviors," in *2020 IEEE-RAS 20th International Conference on Humanoid Robots (Humanoids)*. IEEE, 2021, pp. 1–8.

[27] O. Stasse, T. Flayols, R. Budhiraja, K. Giraud-Esclasse, J. Carpentier, J. Mirabel, A. Del Prete, P. Souères, N. Mansard, F. Lamiraux *et al.*, "Talos: A new humanoid research platform targeted for industrial applications," in *2017 IEEE-RAS 17th International Conference on Humanoid Robotics (Humanoids)*. IEEE, 2017, pp. 689–695.

[28] S. Kuindersma, "Recent progress on atlas, the world's most dynamic humanoid robot," *Robotics Today-A Series of Technical Talks.[Online]. Available: https://youtu. be/EGABAx52GKI*, 2020.

[29] G. A. Castillo, B. Weng, W. Zhang, and A. Hereid, "Robust feedback motion policy design using reinforcement learning on a 3d digit bipedal robot," in *2021 IEEE/RSJ International Conference on Intelligent Robots and Systems (IROS)*. IEEE, 2021, pp. 5136–5143.

[30] I. Radosavovic, T. Xiao, B. Zhang, T. Darrell, J. Malik, and K. Sreenath, "Real-world humanoid locomotion with reinforcement learning," *Science Robotics*, vol. 9, no. 89, p. eadi9579, 2024.

[31] J. Chen, J. Frey, R. Zhou, T. Miki, G. Martius, and M. Hutter, "Identifying terrain physical parameters from vision-towards physical-parameter-aware locomotion and navigation," *IEEE Robotics and Automation Letters*, 2024.

[32] E. J. Hu, Y. Shen, P. Wallis, Z. Allen-Zhu, Y. Li, S. Wang, L. Wang, and W. Chen, "Lora: Low-rank adaptation of large language models," *arXiv preprint arXiv:2106.09685*, 2021.

[33] P. Lewis, E. Perez, A. Piktus, F. Petroni, V. Karpukhin, N. Goyal, H. Küttler, M. Lewis, W.-t. Yih, T. Rocktäschel *et al.*, "Retrieval-augmented generation for knowledge-intensive nlp tasks," *Advances in Neural Information Processing Systems*, vol. 33, pp. 9459–9474, 2020.

[34] G. E. Totten, Ed., *ASM Handbook, Volume 18: Friction, Lubrication, and Wear Technology*. Materials Park, OH: ASM International, 2017. [Online]. Available: https://www.asminternational.org/handbooks/-/journal_content/56/10192/27533578/PUBLICATION

[35] P. J. Blau, *Friction Science and Technology: From Concepts to Applications*, 2nd ed. CRC Press, 2009, https://www.routledge.com/Friction-Science-and-Technology-From-Concepts-to-Applications-Second-Edition/Blau/p/book/9780367386665.

[36] J. Tan, T. Zhang, E. Coumans, A. Iscen, Y. Bai, D. Hafner, S. Bohez, and V. Vanhoucke, "Sim-to-real: Learning agile locomotion for quadruped robots," *arXiv preprint arXiv:1804.10332*, 2018.

[37] K. Sorensen and W. Singhose, "Wheeled inverted pendulum control and slip dynamics," in *2018 IEEE 14th International Conference on Control and Automation (ICCA)*. IEEE, 2018, pp. 336–343.

[38] "Urdf - ros wiki. http://wiki.ros.org/urdf."

[39] A. Dosovitskiy, "An image is worth 16x16 words: Transformers for image recognition at scale," *arXiv preprint arXiv:2010.11929*, 2020.

[40] R. E. Kalman *et al.*, "Contributions to the theory of optimal control," *Bol. soc. mat. mexicana*, vol. 5, no. 2, pp. 102–119, 1960.

[41] J. Schulman, F. Wolski, P. Dhariwal, A. Radford, and O. Klimov, "Proximal policy optimization algorithms," *arXiv preprint arXiv:1707.06347*, 2017.

[42] J. Tobin, R. Fong, A. Ray, J. Schneider, W. Zaremba, and P. Abbeel, "Domain randomization for transferring deep neural networks from simulation to the real world," in *2017 IEEE/RSJ international conference on intelligent robots and systems (IROS)*. IEEE, 2017, pp. 23–30.

[43] G. Ji, J. Mun, H. Kim, and J. Hwangbo, "Concurrent training of a control policy and a state estimator for dynamic and robust legged

locomotion," *IEEE Robotics and Automation Letters*, vol. 7, no. 2, pp. 4630–4637, 2022.

[44] D. Baek, Y.-C. Chang, and J. Ramos, "A study of shared-control with bilateral feedback for obstacle avoidance in whole-body telelocomotion of a wheeled humanoid," *IEEE Robotics and Automation Letters*, 2023.

[45] D. Nistér, O. Naroditsky, and J. Bergen, "Visual odometry," in *Proceedings of the 2004 IEEE Computer Society Conference on Computer Vision and Pattern Recognition, 2004. CVPR 2004.*, vol. 1. Ieee, 2004, pp. I–I.